nzsee
NEW ZEALAND SOCIETY FOR EARTHQUAKE ENGINEERING

Development of LSN-based pipe repair rate models utilising data from the 2011 Christchurch earthquakes

J.M. Moratalla & V.K. Sadashiva
GNS Science, Lower Hutt.

ABSTRACT

The Canterbury Earthquake Sequence adversely impacted built, economic and social environments. This included widespread physical damage to the water supply pipe network in Christchurch, resulting in long service disruptions. The transient and permanent ground deformations generated by the earthquakes, particularly the M_w6.2 22 February 2011 and M_w6.0 13 June 2011 events, caused a range of pipe damage. In some areas the buried water pipes were severely damaged resulting in high repair rates (number of repairs per kilometre of pipe exposed to hazard). Many of the pipe faults were found to be in areas affected by liquefaction and lateral spreading.

Utilising the potable water pipe repair dataset and Liquefaction Severity Number (LSN) maps generated from extensive geotechnical investigation following both the earthquake events, new repair rate models for the water pipes have been derived and are presented in this paper. The proposed models require basic pipe characteristics (pipe size and material type) and LSN results to provide an estimate of repair rate for pipes in potentially liquefiable soil. The models can be easily implemented in a risk modelling tool and used to evaluate the potential damage to buried pipe networks exposed to future earthquake events.

1 INTRODUCTION

As extensively documented in the literature (e.g. BNZSEE 2010; BNZSEE 2011), Christchurch was shaken by a series of strong earthquakes in the period between September 2010 and December 2011. This included the M_w7.1 4th September 2010, M_w6.2 22 February 2011 and M_w6.0 13 June 2011 earthquakes, which caused significant and wide-spread damage to the city's built-environment, including the water supply network (focus of this paper), resulting in service disruptions in the months following the earthquakes. A key characteristic associated with the earthquakes was the strong shaking (see Figure 1) accompanied by wide-spread and severe liquefaction in many areas (Cubrinovski et al. 2011). This resulted in excessive and non-uniform ground deformation such as: large vertical and/or lateral displacements; cracks and fissures in the ground or ground distortion. It was observed that the buried pipes were generally subjected to transient

ground deformations (from shaking) and permanent ground deformations (mostly due to liquefaction effects) often above the capacity of the pipelines to sustain such movements/loads, thereby resulting in wide-spread and numerous pipe faults (i.e. leaks or breaks) (Cubrinovski et al. 2014).

Utilising the pipe repair dataset, and the hazard data relating to the earthquakes, a few studies have proposed pipe fragility models (e.g. Bouziou & O'Rourke 2017; O'Rourke et al. 2014). These models, if they are to be used for forecasting pipe damage, require input parameters that can be difficult to predict and/or measure, or the models are formulated based on only the larger diameter pipes in the network that got damaged in the 22 February 2011 event (Bouziou et. al. 2019; Toprak et al. 2019). New repair rate (i.e. number of pipe repairs/km length) models are developed in this paper utilising repair data of water pipes of all diameter in the network and the Liquefaction Severity Number (LSN) maps generated by Tonkin & Taylor Ltd. (T&T) for the 22 February and 13 June 2011 events. Further details on the steps taken to develop the models are discussed in the following sections.

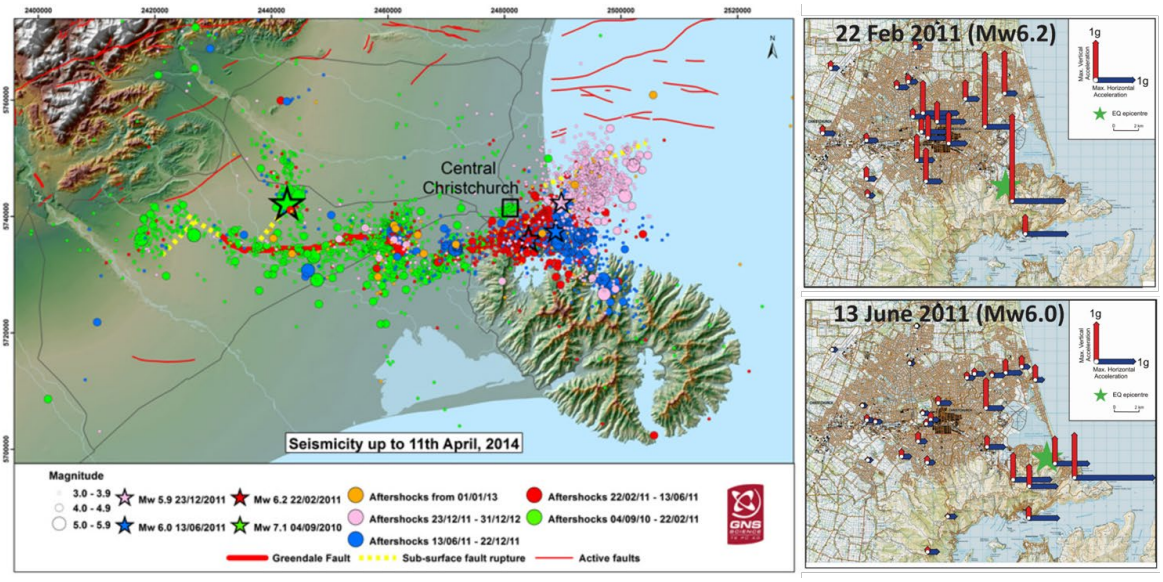

Figure 1: Canterbury Earthquake Sequence (Webb and Kaiser 2012)

2 PIPE NETWORK DATA

Data relating to the Christchurch water supply network, originally collected for a previous study (Sadashiva et al. 2019), was used in this work. The pipe network exposed to the earthquakes was made up of pipes of varying diameter and material types as summarised in Table 1.

Pipe damage information was determined using the repair dataset sourced from City Care Ltd. for the previous study. The repair notes typically contained limited information about the type of repair or cause (i.e. leak or break) but generally contained the inspection dates or repair request dates. This information was helpful to relate an earthquake to an observation of damage and subsequent repair. It also helped to calculate the time taken to restore the network after each event, or the period within which all reported damage could be associated with the event and was not pre-existing damage or damage caused by the previous event in the sequence. O'Rourke et al. (2014) suggest that as the network is restored the cumulative rate of repair (repairs per day) follows a pattern of initial high rate of repair, followed by a transient state with an intermediate repair rate, and finally a steady state of repair with a rate close to the pre-earthquake repair rates (i.e. 'business as usual'). The beginning of the steady state of repair is considered to show where the repair period associated with the event ends. This tri-linear trend was able to be identified in the collected repair data. For the 22nd February 2011 earthquake, the change to a steady state of repair was found to occur around 15th April 2011; therefore, repairs identified in the inspection process before 15th April 2011 were

considered pipe faults related to the February earthquake. For the June event, the onset of transition to the steady state occurred approximately two months after the earthquake.

Table 1: Summary of potable water pipes in the network (Sadashiva et al. 2020)

Pipe material	Pipe diameter <75mm		Pipe diameter ≥75mm	
	km	% Total Length	km	% Total Length
Asbestos Cement (ND*) – AC	18.2	1.1	884.6	49.8
Concrete Lined Steel (D*) – CLS	-	-	56.5	3.2
Ductile Iron (D*) – DI	0.2	0.01	51.4	2.9
Cast Iron (ND*) – CI	0.5	0.03	226.6	12.8
Modified Polyvinyl Chloride (D*) – MPVC	0.6	0.03	141.8	8.0
Polyvinyl Chloride (D*) – PVC	66.4	3.9	206.0	11.6
Steel (D*) – S	0.4	0.02	50.1	2.8
Unplasticized Polyvinyl Chloride (D*) – UPVC	2.2	0.1	113.4	6.4
Galvanised Iron – GI (ND*)	208.3	12.1	3.7	0.2
High Density Polyethylene (D*) – HDPE	921.5	53.5	1.7	0.1
Med. Density Polyethylene – MDPE80 (D*)	458.9	26.6	2.8	0.2
Other (also includes unknown pipe type)**	46.9	2.7	36.5	2.1
TOTAL	**1724.1**	**100.0**	**1775.2**	**100.0**

*Ductile (D) or Non-Ductile (ND). **Mixed material ductility.

3 LIQUEFACTION SEVERITY NUMBER (LSN) MAPS

Much of the earthquake damage to Christchurch's built environment was caused by permanent ground damage, including liquefaction and lateral spreading in areas close to rivers, wetlands and estuaries. Extensive studies were undertaken following the earthquakes to assess the vulnerability of land to liquefaction damage on the flat land and lateral spreading damage (see Maurer et al. 2015; T&T 2013, 2015; van Ballegooy et al. 2014, 2015b). Data from over 25,000 Cone Penetration Tests (CPT), laboratory testing along with groundwater data from hundreds of monitoring wells, were used to characterise land vulnerability to the liquefaction hazard. Of the CPT-based liquefaction vulnerability indices evaluated and comparative studies carried out by T&T, it was found that Liquefaction Severity Number (LSN) index provided the strongest correlation with land damage observations during the Canterbury Earthquake Sequence (van Ballegooy et al. 2014, 2015a, 2015b).

LSN reflects calculated volumetric densification strain within different layers of soil, weighted by depth, as a proxy for likely severity of liquefaction land damage at the surface. It is calculated as the summation of the post-liquefaction volumetric reconsolidation strains calculated for each soil layer divided by the depth to the midpoint of that layer. The value of LSN is theoretically between 0 (for no liquefaction vulnerability) to a large number (e.g. greater than 60, for extreme liquefaction vulnerability). More details on the above can be found in the literature (e.g. T&T 2013, 2015; van Ballegooy et al. 2014, 2015b). Liquefaction-related lateral

displacements (phenomena known as lateral spreading) are not represented by LSN since horizontal movements are dependent on the slope and the distance to a free face (Zhang et al, 2004), pipe damage directly related to lateral spreading was excluded from the pipe repair models.

LSN maps relating to the 22 February and 13 June 2011 events were provided by T&T as GIS raster files the 50th percentile LSN value maps (Figure 2) were used for repair rate model development. Given that LSN calculations include ground shaking intensities (PGA), magnitude and groundwater conditions, the expected level of ground damage for a given LSN value is consistent between earthquakes, being this a major advantage that allows combining damage datasets from different events.

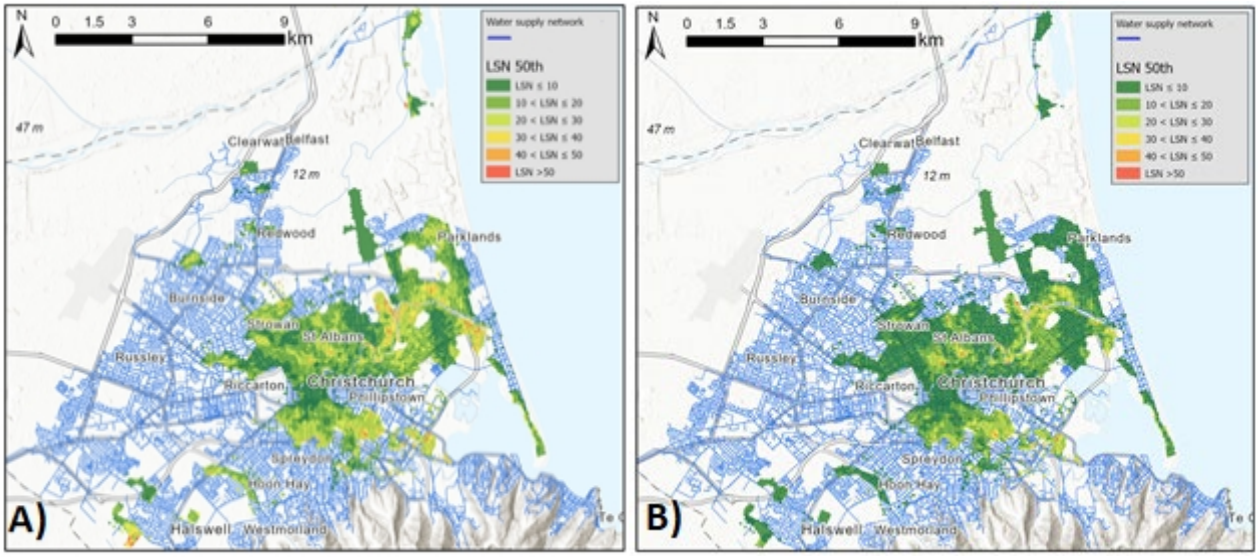

Figure 2: Potable water pipe network data overlaid on map of 50th percentile LSN for the A) 22nd February and B)13th June 2011 earthquakes affecting Christchurch..

4 PIPE FRAGILITY MODEL DEVELOPMENT

LSN based repair rate functions (or models) were developed in the following way. The repair data and the LSN values relating to the 22 February and 13 June 2011 earthquakes were first geospatially joined to the pipe network data. Here, only pipe segments where LSN was greater than zero were considered (see **Error! Reference source not found.** for pipe statistics in LSN >0 zone relating to the February event) for model development. The repair dataset was then divided into LSN bins of equal size and repair rate (RR) calculated by dividing the number of pipe repairs over the total length of the pipe within each bin. In order to remove extreme repair rates that can arise from low sample sizes (i.e. short total lengths), the calculated repair rates were then put through a screening criterion (described in O'Rourke et al. 2014). The screening method assumes the damage data follows a Poisson distribution and defines the minimum sample length required for using the grouped data with a confidence interval of 90% and a standard deviation of 50%. We developed an optimisation algorithm to maximize the number of data points included in each regression. The algorithm iterates through all possible LSN bin sizes and selects the minimum bin size where all the points pass the screening criteria. Figure 3 shows the points for pipes of different materials that passed the screening criteria for a LSN bin of size 12 The figure shows that the repair rates typically increase with liquefaction severity, and that the non-ductile pipes sustained more damage than pipes made of ductile material. Also, consistent with damage observations, the February event typically caused more damage to the pipes (resulting in higher repair rates) than the June event.

As explained in section 2, the ground damage associated to the calculated LSN values should be consistent between earthquakes. In order to reduce the bias in the relationships, we combined both February and June

damage data into a single dataset, increasing the exposure length for deriving the models. We also developed models using only the February dataset (the more damaging event). Several regression methods (linear, exponential, polynomial and natural log) were explored to fit the LSN-RR datapoints; they all generally provided reasonably good fits. Due to the clear linear trend observed in the data points, and because Ordinary Least Squares (OLS) linear fit was found to provide smaller standard deviation on the residuals than other options, the OLS method was chosen to develop the repair rate functions.

Table 2: Number of pipe repairs and pipe lengths (in km) in LSN >0 areas: Mw6.2 22 February 2011 earthquake (see Figure 2). Note that only selected pipe material types are tabulated here.

Pipe material	Pipe diameter <75mm			Pipe diameter ≥75mm		
	km (%*)	No. of repairs (%**)	Repair Rate (unscreened)	km (%*)	No. of repairs (%**)	Repair Rate (unscreened)
AC	0.8 (4.5)	1 (25)	1.21	216.3 (24.4)	715 (70)	3.31
CLS	-	-	-	26.8 (47.5)	47 (84)	1.75
DI	0.02 (12.9)	-	-	22.1 (42.9)	25 (81)	1.13
CI	0.2 (43.4)	-	-	98.6 (43.5)	165 (65)	1.67
MPVC	0.02 (4.4)	-	-	27.9 (19.7)	11 (85)	0.39
PVC	7.6 (11.5)	3 (20)	0.39	72.8 (35.3)	50 (79)	0.69
Steel	0.1 (23.8)	-	-	19.8 (39.4)	19 (61)	0.96
UPVC	0.1 (3.1)	-	-	21.2 (18.7)	7 (41)	0.33
GI	90 (43.2)	645 (67)	7.16	0.1 (2.4)	-	-
HDPE	332 (36)	255 (56)	0.77	1.1 (62.3)	-	-
MDPE80	134.4 (29.3)	69 (70)	0.51	0.8 (26.6)	-	-

*Pipe length proportion with respect to corresponding pipe type total length in the network (see Table 1).
**Number of pipe repairs proportion with respect to corresponding pipe type total repairs in the network.

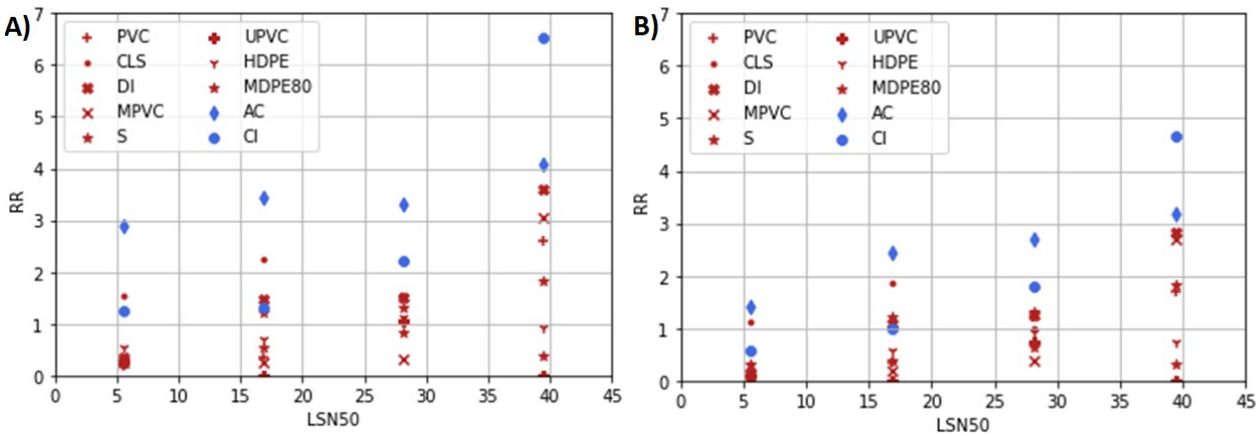

Figure 3: Mean repair rates vs. LSN using: A) 22 February 2011 event dataset; B) 22 February and 13 June 2011 event combined dataset. Ductile and non-ductile materials are respectively shown in red and blue.

4.1 General Repair Rate models

Prior to developing RR models for pipes of specific material, RR models for pipes grouped by combination of diameter (i.e. $\phi < 75$mm or $\phi \geq 75$mm) and material type (i.e. ductile or non-ductile, see Table 1) were derived. A large proportion of non-ductile pipes of diameter less than 75mm in the network is represented by Galvanised Iron (GI) pipes. These pipes performed poorly during the earthquakes and had repair rates more than 10 times the mean repair rates of pipes of other materials. Therefore, GI pipes were excluded from the grouping and a separate class was created for them. Enough LSN-RR data points passed the screening criteria and became available for RR models for Ductile and Non-ductile pipes with $\phi \geq 75$mm, and for Ductile pipes with $\phi < 75$mm (see Figures 4 and 5a). Repair rate models for GI pipes were also derived and are shown in Figure 5b.

In addition to the above, a 'generic' repair rate model was derived from combining all material types except GI pipes in the $\phi \geq 75$mm group dataset. This model (shown in Figure 4) can potentially be useful to estimate repair rate in cases where no information on the pipe material is available for pipe damage modelling. To avoid bias due to differences in lengths of different materials (i.e. avoid those materials with larger total lengths to have more weight in the generic equation), this model was derived using the weighted mean data-pairs calculated for the ductile and non-ductile material groups. The general form of the repair rate models is shown by Equation 1. The value of the parameters a_0 and b_0, and the standard deviation of the residuals (σ_m) for each model is provided in Table 3.

$$RR = a_0 + b_0 LSN \quad (1)$$

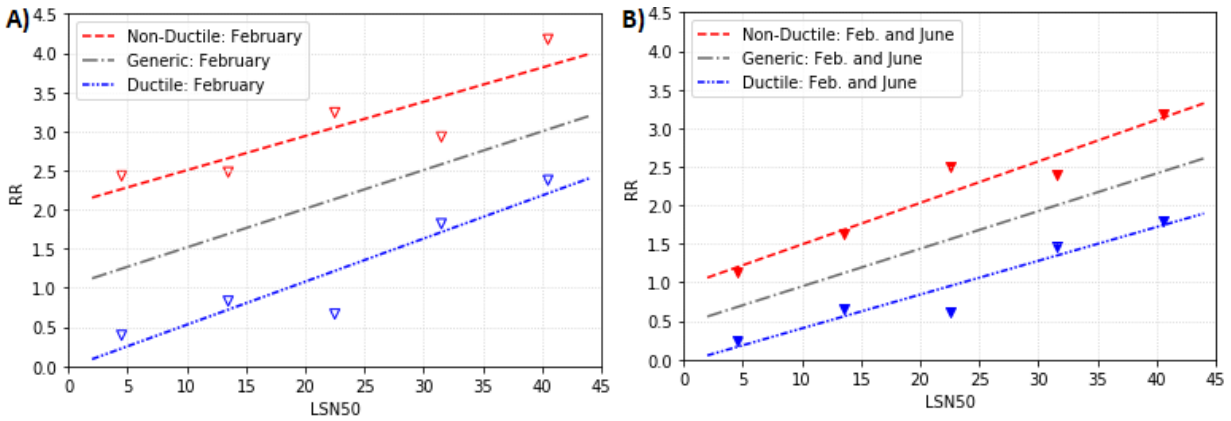

Figure 4: Repair Rate (RR) models for pipes of diameters ≥ 75mm using: A) 22 February 2011 event dataset; B) 22 February and 13 June 2011 events combined dataset. Triangles represent the data points used in the regressions.

Table 3: Equation (1) parameter values. σ_m is the uncertainty associated with the regression (i.e. standard deviation of the residuals)

22 February event dataset

Diameter group	Material group	a_0	b_0	σ_m
≥75mm	Generic	1.023	0.049	0.965
	Ductile	-0.02	0.055	0.277
	Non-ductile	2.065	0.044	0.308
<75mm	Ductile	0.301	0.023	0.062
	Galvanised Iron	3.950	0.205	0.702

22 February and 11 June event combined dataset				
Diameter group	**Material group**	**a_0**	**b_0**	**σ_m**
≥75mm	Generic	0.460	0.049	0.637
	Ductile	-0.034	0.044	0.173
	Non-ductile	0.954	0.054	0.192
<75mm	Ductile	0.129	0.022	0.153
	Galvanised Iron	1.4591	0.2331	0.644

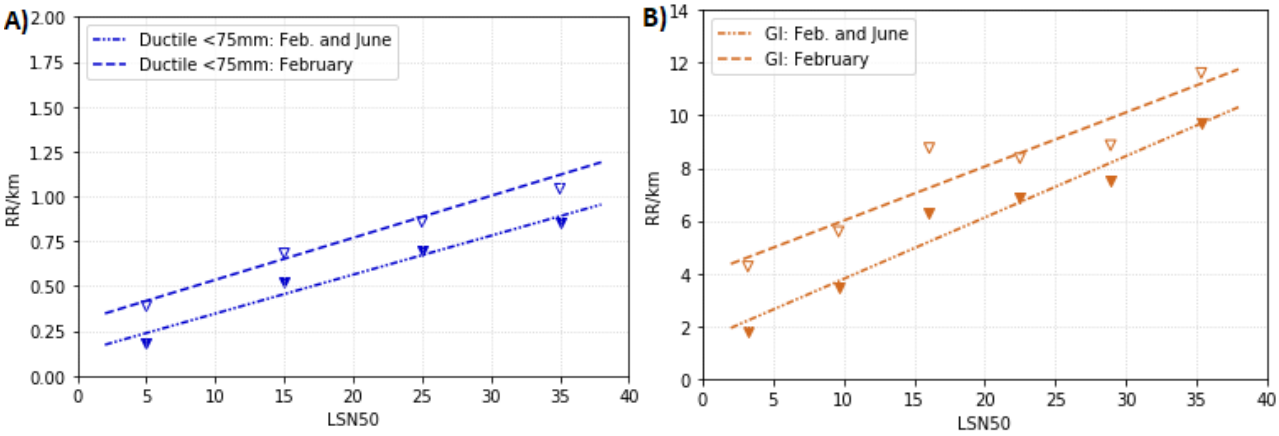

Figure 5: Repair Rate (RR) models for pipes of diameters <75mm: A) Ductile pipes; B) Galvanised Iron pipes

4.2 Material-specific Repair Rate models

In order to develop RR models for pipes of specific material, we derived correction factors for the general relationships for AC, CI, PVC, HDPE and MDPE80 pipes. The correction factors were derived by fitting the residuals between the generic relationships and the datapoints for the analysed material type. The screening criteria was again applied here to ensure the minimum sample size requirement was met.

The general form of the corrected repair rate model Equation 2.The correction factors are included in table 4, here a_1 and b_1 are the material-specific correction factors and a_0 and b_0 are the factors from Table 3. The repair rate models are shown in Figure 6 and Figure 7.

$$RR = a_0 + b_0 LSN + a_1 + b_1 LSN \quad (2)$$

Table 4: Equation (2) parameter values. σ_m is the uncertainty associated to the regression (i.e. standard deviation of the residuals).

22 February event dataset						
Diameter group	**Material group**	**a_0**	**b_0**	**a_1**	**b_1**	**σ_m**
≥75mm	AC	2.065	0.044	0.764	-0.018	0.303
	CI	2.065	0.044	-1.393	0.023	0.402
	PVC	-0.02	0.055	-0.827	0.046	0.583
<75mm	HDPE	0.301	0.023	0.028	0.004	0.075
	MDPE80	0.301	0.023	-0.125	-0.004	0.142

22 February and 11 June event combined dataset

Diameter group	Material group	a_0	b_0	a_1	b_1	σ_m
≥75mm	AC	0.954	0.054	0.462	-0.01	0.266
	CI	0.954	0.054	-0.841	0.011	0.23
	PVC	-0.034	0.044	-0.595	0.03	0.322
<75mm	HDPE	0.129	0.022	0.024	0.004	0.136
	MDPE80	0.129	0.022	-0.122	-0.002	0.058

Among the non-ductile pipes of diameter ≥75mm, the repair rate results in Figure 6 show AC pipes were more vulnerable to liquefaction effects than the CI pipes. The PVC pipes (ductile category) of diameter ≥75mm show lower repair rates than the AC and CI pipes. The above observation can be seen in results obtained using February dataset only, as well as when the February and June combined dataset is used. From the pipe group of diameters <75mm and made of ductile material, MDPE80 pipes show lower repair rates than pipes of HDPE material (see Figure 7).

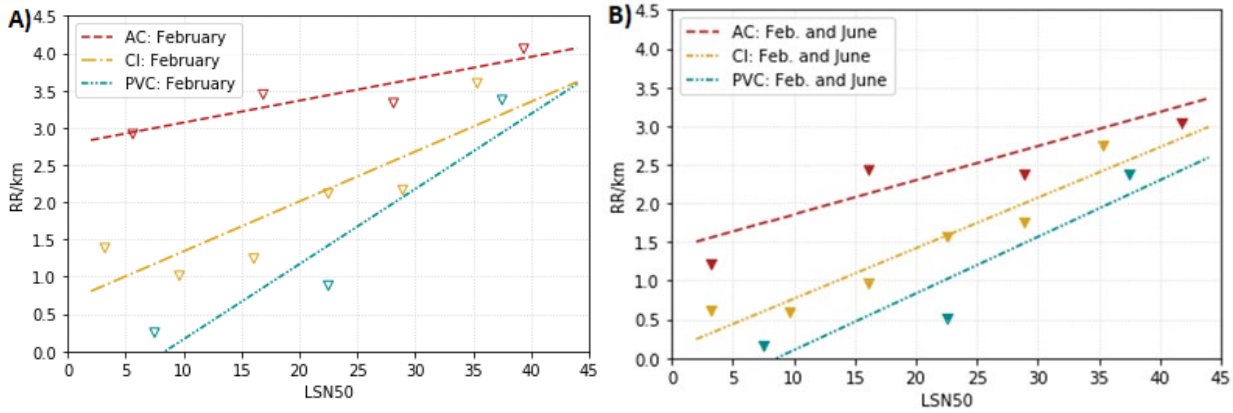

Figure 6: Repair Rate (RR) models for AC, CI and PVC material pipes of diameter ≥75mm using: A) February event dataset; B) February and June events combined.

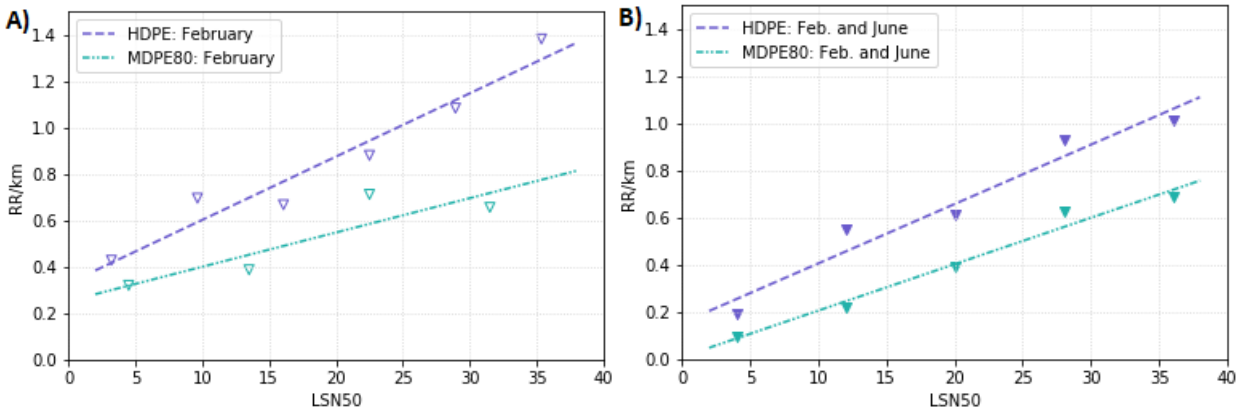

Figure 7: Repair Rate (RR) model for pipes of diameter <75mm and made of HDPE and MDPE80 materials. A) February event dataset; B) February and June event combined dataset

The uncertainty of the material-corrected models (σ_m) was obtained by calculating the standard deviation of the residuals between the corrected models and the datapoints for pipes of specific materials. A boxplot of the residuals (difference between observed data and the model) for all the repair rate functions derived in this

study is shown in Figure 8. Combining the two event datasets increases the exposure length of each diameter group and material type, producing a general reduction of the uncertainty in the models. CI and PVC pipes showed the most significant uncertainty reduction by combining datasets.

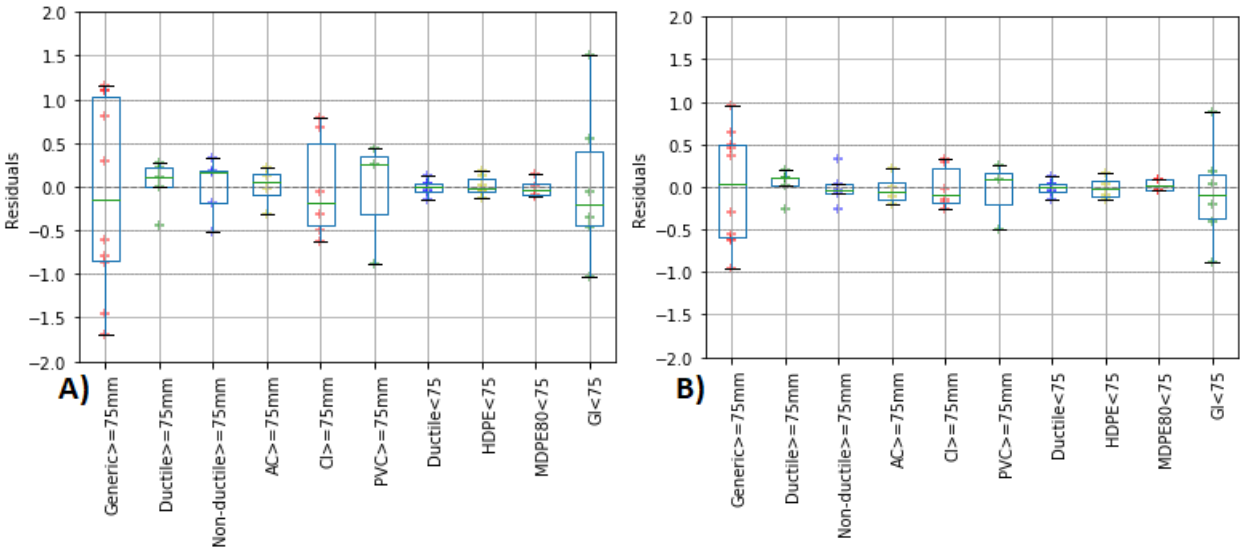

Figure 8: Boxplot of the residuals resulting from each model. A) 22 February 2011 event dataset and B) 22 February and 13 June 2011 event combined dataset

5 CONCLUSIONS

The transient and permanent ground deformations generated by the M_w6.2 22 February and M_w6.0 13 June 2011 Christchurch earthquakes severely damaged buried water pipes in some areas of the city resulting in high repair rates (number of repairs per kilometre of pipe exposed to hazard). Most of the damage to the pipes was attributed to liquefaction and lateral spreading effects. Pipes made of ductile material (e.g. PVC, HDPE) sustained lesser damage (and therefore lower repair rates) compared to the pipes made of non-ductile material (e.g. AC, CI). In all cases, the repair rates typically increased with increasing liquefaction severity.

Utilising the Liquefaction Severity Number (LSN) maps obtained for the 50th percentile of the Cyclic resistance ratio (CRR)and pipe repair data relating to the two events, new repair rate models were developed and presented in this paper. A minimum sample length was defined by applying a screening criteria assuming a Poisonian distribution on the data with 95% confidence and a standard deviation of 0.5..
Two sets of models were derived in this study using: damage data from the February event, and damage data from the combined damage datasets from February and June. The consistency between LSN calculations between events permitted combining the damage data from February and June, extending the sample length and reducing the uncertainties in the regressions (i.e. standard deviation of the Least Squares fit selected).

General repair rate functions were derived from pipes grouped by combination of diameter (i.e. $\phi < 75$mm or $\phi \geq 75$mm) and material type (i.e. ductile or non-ductile). The general models were refined by adding correction factors for those material types with sufficient sample length, enabling material-specific repair rate models to be developed for AC, CI, PVC pipes of diameter ≥75mm and for MDPE and HDPE80 pipes of diameter <75mm. Galvanised Iron pipes performed poorly during the earthquakes, resulting in very high repair rates compared to the other non-ductile pipes of <75mm damaged in the network; this warranted a separate repair rate model to be developed for this pipe type. The proposed repair rate models can be used to estimate the number of pipe repairs on buried water pipes due to potential liquefaction damage from future earthquakes.

6 ACKNOWLEDGEMENTS

The authors thank Sjoerd van Ballegooy and Virginie Lacrosse of Tonkin & Taylor Ltd for providing the LSN maps. Pipeline and damage data collected for an earlier study was utilised in this work; SCIRT, City Care Ltd., Opus Research are thanked. The authors are also thankful to their colleagues: Giovanni Pradel, David Heron and Biljana Lukovic for their help with GIS work, and David Rhoades and Sally Dellow for their review comments and suggestions on the paper. Funding support for this work is from GNS Science HRM SSIF project: *Built Environment & Performance, Social Vulnerability, Evolving Landscapes Project*.

REFERENCES

Bouziou, D. & O'Rourke, T.D. 2017. Response of the Christchurch water distribution system to the 22 February 2011 earthquake, *Soil Dynamics and Earthquake Engineering*, Vol 97: 14-24.

Bouziou, D., van Ballegooy S., Storie. L & O'Rourke, T.D. 2019. *Spatial correlations of underground pipeline damage in Christchurch.* Christchurch: UC QuakeCentre.

Bulletin of the New Zealand Society for Earthquake Engineering, 43(4). 2010. Accessed November 20, 2020. http://www.nzsee.org.nz/bulletin_index/43_4.htm

Bulletin of the New Zealand Society for Earthquake Engineering, 44(4). 2011. Accessed November 20, 2020. http://www.nzsee.org.nz/bulletin_index/44_4.htm

Cubrinovski, M., Bradley, B., Wotherspoon, L. DePascale, G., & Wells, D. 2011. Geotechnical aspects of the 22 February 2011 Christchurch earthquake, *Bulletin of the New Zealand Society for Earthquake Engineering*, 44(4): 205-226.

Cubrinovski, M., Hughes, M., Rourke. T. 2014. Impacts of liquefaction on the potable water system of Christchurch in the 2010–2011 Canterbury (NZ) Earthquakes, *Journal of Water Supply: Research and Technology – AQUA*, Vol 63(2): 95-105.

Maurer BW, Green RA, Taylor O-DS. 2015. Moving towards an improved index for assessing liquefaction hazard: Lessons from historical data, *Soils and Foundations, JGS*, 55(4): 778-787.

O'Rourke, T.D., Jeon, S-S., Toprak, S., Cubrinovski, M., Hughes, M., van Ballegooy, S., Bouziou, D. 2014. Earthquake response of underground pipeline networks in Christchurch, NZ, *Earthquake Spectra*, Vol 30(1): 183-204.

Sadashiva, V.K. (comp.), Nayyerloo, M., Sherson, A.K. 2019. *Seismic performance of underground water pipes during the Canterbury Earthquake Sequence*. Lower Hutt: GNS Science. (Consultancy Report 2017/188).

Sadashiva, V.K., Nayyerloo, M., Sherson, A. 2020. Simple buried pipeline fragility models based on data from the 2011 Canterbury earthquakes. In *21st Symposium of the New Zealand Geotechnical Society*. Wellington: Institute of Professional Engineers New Zealand.

Tonkin & Taylor (T&T). 2013. *Liquefaction vulnerability study*. Report prepared for Earthquake Commission, February 2013. Wellington: Tonkin and Taylor. (T+T report; 52020.0200/v1.0).

Tonkin & Taylor (T&T) 2015. *Canterbury Earthquake Sequence: Increased Liquefaction Vulnerability Assessment Methodology*. Report prepared for the Earthquake Commission. Wellington: Tonkin and Taylor. (52010.140/v1.0).

Toprak, S., Nacaroglu, E., van Ballegooy, S., Koc, A.C., Jacka, M., Manav, Y., Torvelainen, E., O'Rourke, T.D. 2019. Segmented pipeline damage predictions using liquefaction vulnerability parameters, *Soil Dynamics and Earthquake Engineering*, Vol 125: 105758.

van Ballegooy, S., Green, R.A., Lees, J., Wentz, R., Maurer, B.W. 2015a. Assessment of various CPT based liquefaction severity index frameworks relative to the Ishihara (1985) H1-H2 boundary curves, *Soil Dynamics and Earthquake Engineering*, 79(B): 347-364.

van Ballegooy, S., Malan, P., Lacrosse, V., Jacka, M.E., Cubrinovski, M., Bray, J.D., O'Rourke, T.D., Crawford, S.A., Cowan, H. 2014. Assessment of liquefaction-induced land damage for residential Christchurch, *Earthquake Spectra*, 30(1): 31-55.

van Ballegooy, S., Wentz, F., Boulanger, R.W. 2015b. Evaluation of a CPT-based liquefaction procedure at regional scale, *Soil Dynamics and Earthquake Engineering*, 79(B): 315-334.

Webb, T.H., Kaiser, A.E. 2012. Update to GNS Science/University of Canterbury July 2011 Report to the Royal Commission. Lower Hutt: GNS Science. (GNS Science consultancy report 2012/94LR). https://canterbury.royalcommission.govt.nz/documents-by-key/20120410.4075/$file/SEI.GNS.0021.pdf